

Crystal structure of clofarabine (form I), $C_{10}H_{11}ClFN_5O_3$, from synchrotron power diffraction data and density functional theory calculations

Jacob K. Salazar,^a James A. Kaduk,^{b,c*} Anja Dosen^d and Thomas N. Blanton^e

Received 30 April 2026

Accepted 22 June 2026

Edited by W. T. A. Harrison, University of Aberdeen, United Kingdom

Keywords: powder diffraction; clofarabine; Clolar; Rietveld refinement; density functional theory.

CCDC references: 2564142; 2564141

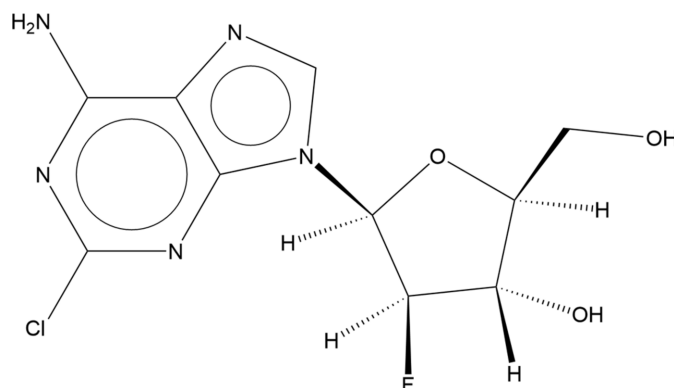
Supporting information: this article has supporting information at journals.iucr.org/e

^aNorth Central College, Department of Chemistry, 131 S. Loomis St., Naperville IL 60540, USA, ^bNorth Central College, Department of Physics, 131 S. Loomis St., Naperville IL 60540, USA, ^cDepartment of Chemistry, Illinois Institute of Technology, 3101 S. Dearborn St., Chicago IL 60616, USA, ^dICDD, 12 Campus Blvd., Newtown Square, PA 19073-3273, USA, and ^eICDD, 12 Campus Blvd., Newtown Square, PA 19073-3273, USA. *Correspondence e-mail: kaduk@polycrystallography.com

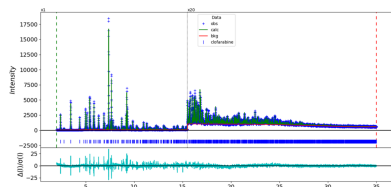
The crystal structure of clofarabine (form I) [systematic name: 2-chloro-9-(2-deoxy-2-fluoro- β -D-arabinofuranosyl)-9H-purin-6-amine], $C_{10}H_{11}ClFN_5O_3$, has been solved and refined using synchrotron X-ray powder diffraction data, and optimized using density functional theory techniques. The oxolane ring adopts an envelope conformation and the angle between the mean ring planes is $88.4(2)^\circ$, resulting in an L-shaped molecule. The molecules stack along the short a -axis direction, and N—H \cdots O, O—H \cdots N and N—H \cdots N hydrogen bonds link them into a three-dimensional network.

1. Chemical context

Clofarabine, $C_{10}H_{11}ClFN_5O_3$ (marketed as Clolar, Evoltra and Clofarex in different countries) is a purine nucleoside antimetabolite, used to treat relapsed or refractory acute lymphoblastic leukemia in children and young adults (Bonate *et al.*, 2006). Clofarabine is administered intravenously and functions by inhibiting DNA synthesis and ribonucleoside reductase. The systematic name (CAS Registry Number 123318-82-1) is (2*R*,3*R*,4*S*,5*R*)-5-(6-amino-2-chloropurin-9-yl)-4-fluoro-2-(hydroxymethyl)oxolan-3-ol.



A powder pattern for clofarabine (form I) has been reported in Chinese Patent CN101407640A (Xia *et al.*, 2011). Un-named crystalline forms of clofarabine are claimed in US Patent 5,034,518 (Montgomery & Secrist, 1991; Southern Research Institute) and US Patent 5,661,136 (Montgomery & Secrist, 1997; Southern Research Institute). Xia *et al.* suggest



OPEN ACCESS

Published under a CC BY 4.0 licence

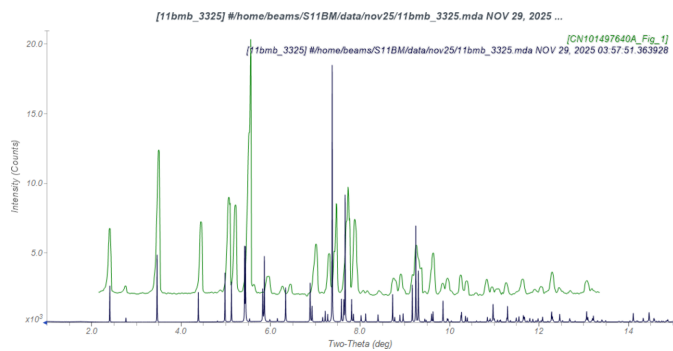


Figure 1
Comparison of the synchrotron pattern of clofarabine Form I (black) to that reported by Xia *et al.* (2011) using Cu $K\alpha$ radiation (green) converted to the synchrotron wavelength of 0.4687342 Å. The patent pattern (measured using Cu $K\alpha$ radiation) was digitized using *UN-SCAN-IT* (Silk Scientific, 2013) and converted to the synchrotron wavelength of 0.4687342 Å using *JADE Pro* (MDI, 2025). Image generated using *JADE Pro* (MDI, 2025).

that these earlier forms were monohydrates, and claim that their form is new. The present work was carried out as part of a project (Kaduk *et al.*, 2014) to determine the crystal structures of large-volume commercial pharmaceuticals, and includes high-quality powder diffraction data for them in the Powder Diffraction File (Kabekkodu *et al.*, 2024).

2. Structural commentary

The synchrotron X-ray powder pattern of clofarabine is similar enough to that reported by Xia *et al.* (2011) for form I (Fig. 1) to conclude that they represent the same material. The patent pattern exhibits significant displacement/transparency peak position errors, as well as substantial preferred orientation.

The mean plane of the C16–C20/N6–N9 purine ring system of the asymmetric molecule lies approximately in the (122) Miller plane, and the mean plane of the C11–C14/O3 oxolane ring is aligned approximately with (122). The latter ring adopts an envelope conformation with atom C12 as the flap. The angle between the mean ring planes is 88.4 (2)°, so the mol-

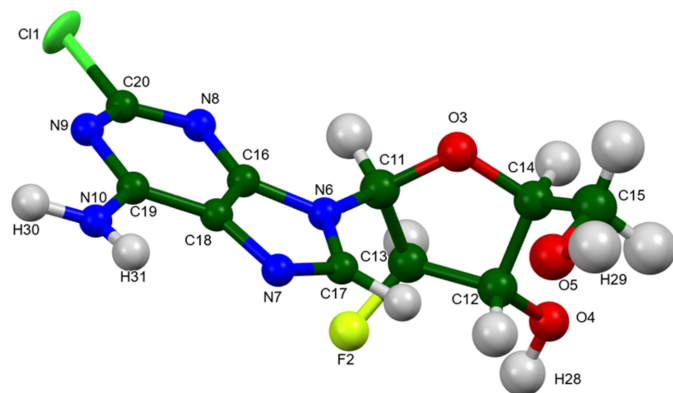


Figure 2
The molecular structure of clofarabine, showing 50% probability spheroids/ellipsoids.

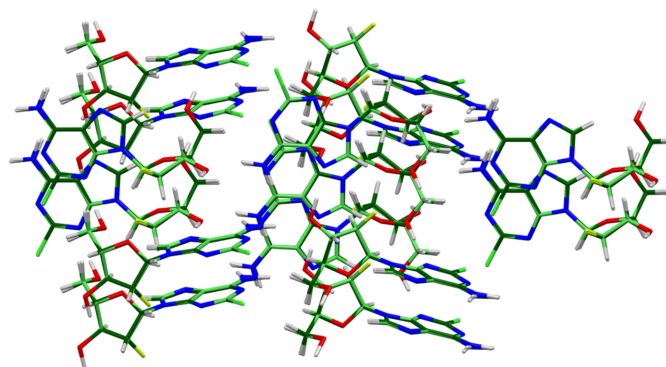


Figure 3
Comparison of the Rietveld-refined (colored by atom type) and *VASP*-optimized (pale green) structures of clofarabine, calculated using the *Mercury* CSD-Materials/Search/Crystal Packing Similarity tool. The root-mean-square Cartesian displacement is 0.078 Å.

ecules may be described as L-shaped (Fig. 2). The root-mean-square difference of the non-H atoms in the Rietveld-refined and *VASP*-optimized structures of clofarabine, calculated using the *Mercury* (Macrae *et al.*, 2020) CSD-Materials/search/crystal packing similarity tool is 0.078 Å (Fig. 3); the structures are essentially identical. The root-mean-square Cartesian displacement of the non-H atoms in the refined and optimized structures, calculated using the *Mercury* Calculate molecule overlay tool, is 0.048 Å (Fig. 4). The agreements are within the normal range for correct structures (van de Streek & Neumann, 2014). The remaining discussion will emphasize the *VASP*-optimized structure.

All of the bond distances, bond angles, and torsion angles fall within the normal ranges indicated by a *Mercury* Mogul geometry check (Macrae *et al.*, 2020). Quantum chemical geometry optimization of the isolated clofarabine molecule (DFT/B3LYP/6-31G*/water) using *Spartan '24* (Wavefunction, 2025) indicated that the observed conformation is 5.2 kcal mol⁻¹ higher in energy than a local minimum, which has a very similar conformation. The global minimum-energy conformation is 14.8 kcal mol⁻¹ lower in energy, but is folded on itself to form intramolecular O–H...N hydrogen bonds. Intermolecular interactions are thus important in determining the observed solid-state conformation.

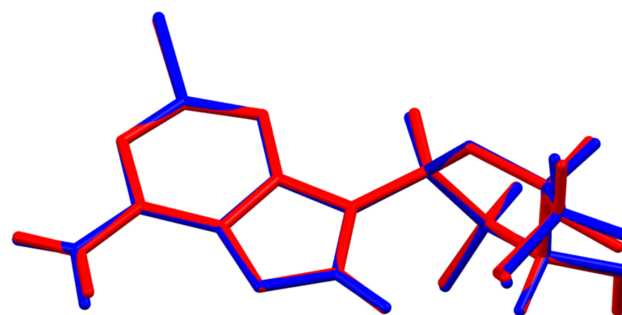


Figure 4
Comparison of the refined structure of clofarabine (red) to the *VASP*-optimized structure (blue). The comparison was generated using the *Mercury* Calculate/Molecule Overlay tool; the r.m.s. difference is 0.048 Å.

Table 1

Hydrogen-bond geometry (Å, °) for clofarabine_VASP.

$D-H\cdots A$	$D-H$	$H\cdots A$	$D\cdots A$	$D-H\cdots A$
O4—H28 \cdots N7 ⁱ	1.01	1.72	2.726	173
O5—H29 \cdots N8 ⁱⁱ	0.99	1.86	2.831	167
N10—H30 \cdots O4 ⁱⁱⁱ	1.03	1.87	2.854	159
N10—H31 \cdots N10 ^{iv}	1.02	2.38	3.271	145
C11—H21 \cdots F2 ^v	1.10	2.27	3.208	142
C11—H21 \cdots O5 ^{vi}	1.10	2.60	3.531	142
C12—H22 \cdots O3 ^{vii}	1.10	2.40	3.396	149
C15—H26 \cdots CH ^{viii}	1.11	2.77	3.570	129
C17—H27 \cdots F2 ^{ix}	1.09	2.40	3.177	127

Symmetry codes: (i) $-x+2, y+\frac{1}{2}, -z+\frac{1}{2}$; (ii) $-x+1, y-\frac{1}{2}, -z+\frac{1}{2}$; (iii) $-x+\frac{3}{2}, -y, z-\frac{1}{2}$; (iv) $x+\frac{1}{2}, -y-\frac{1}{2}, -z$; (v) $x-1, y, z$; (vi) $-x+1, y+\frac{1}{2}, -z+\frac{1}{2}$; (vii) $x+1, y, z$; (viii) $-x+\frac{1}{2}, -y, z+\frac{1}{2}$; (ix) $-x+2, y-\frac{1}{2}, -z+\frac{1}{2}$.

3. Supramolecular features

Viewed down the short a -axis direction (Fig. 5) the structure exhibits discrete clofarabine molecules. When viewed down the c -axis direction (Fig. 6) a herringbone arrangement of molecules is apparent. The shortest ring centroid–ring centroid distance is 5.067 (2) Å, as the molecules stack along the a -axis direction.

Analysis of the contributions to the total crystal energy of the structure using the Forcite module of *Materials Studio* (Dassault Systèmes, 2025) indicated that the intramolecular energy is dominated by angle distortion terms, as might be expected for a molecule containing a fused ring system. The intermolecular energy is dominated by van der Waals attractions, which in this force-field based analysis include hydrogen bonds. The hydrogen bonds are better discussed using the results of the DFT calculation.

There are several hydrogen bonds in the structure (Table 1). The amino group N10 acts as a donor in two classical hydrogen bonds, one to the hydroxyl group O4 and to another amino group N10. The energy of the N10—H30 \cdots O4 hydrogen bond is 5.6 kcal mol⁻¹, calculated using the correlation of Wheatley & Kaduk (2019). The hydroxyl groups O4 and O5 form strong O—H \cdots N hydrogen bonds to the ring N atoms N7 and N8, respectively. These link the molecules into chains along the b -axis direction, with graph set descriptors (Etter, 1990; Bernstein *et al.*, 1995; Motherwell *et al.*, 2000) $C_1^1(8)$, $C_1^1(9)$ and $C_2^2(11)$. The N—H \cdots O and N—H \cdots N hydrogen bonds link the molecules along the c -axis direction, with graph sets $C_1^1(10)$ and $C_1^1(2)$. These and other larger patterns result in a three-dimensional hydrogen bond network. Four intra- and inter-molecular C—H \cdots O hydrogen bonds also contribute to the lattice energy.

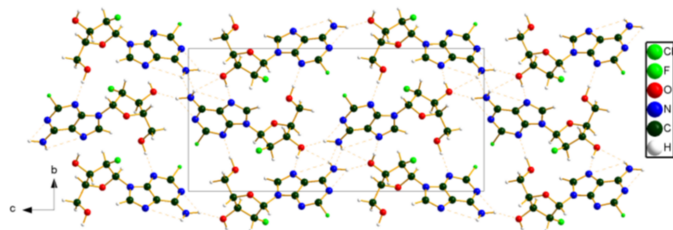


Figure 5
Crystal structure of clofarabine, viewed down the a axis.

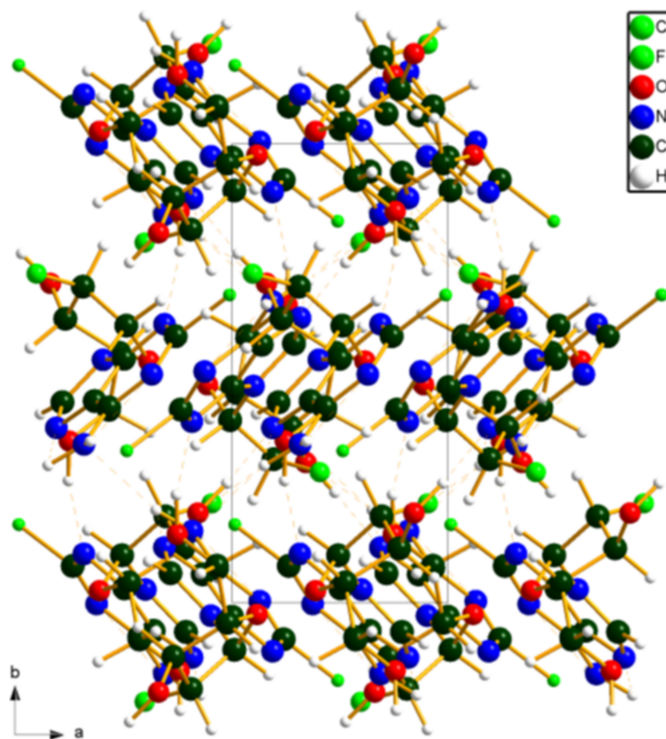


Figure 6
Crystal structure of clofarabine, viewed down the c axis.

The volume enclosed by the Hirshfeld surface of clofarabine (Fig. 7; Hirshfeld, 1977; Spackman *et al.*, 2021) is 299.22 Å³ or 97.94% of 1/4 of the unit-cell volume. The packing density is thus typical. The only significant close contacts (red in Fig. 9) involve the hydrogen bonds. The volume/non-hydrogen atom is smaller than normal, at 15.3 Å³.

The Bravais–Friedel–Donnay–Harker (Bravais, 1866; Friedel, 1907; Donnay & Harker, 1937) algorithm suggests that we might expect elongated morphology for crystallites of clofarabine, with [100] as the long axis. A second-order

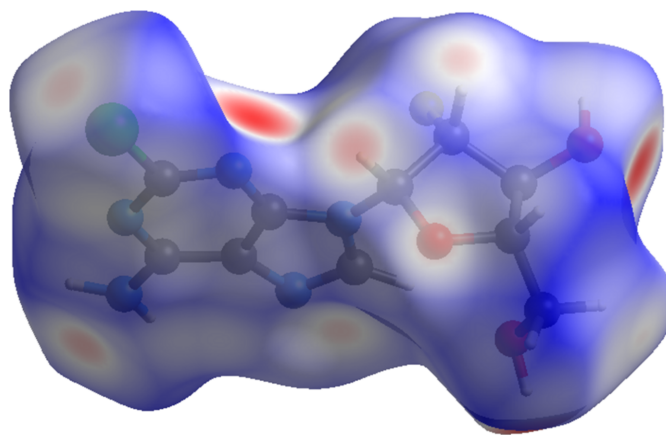


Figure 7
The Hirshfeld surface of clofarabine. Intermolecular contacts longer than the sums of the van der Waals radii are colored blue, and contacts shorter than the sums of the radii are colored red. Contacts equal to the sums of radii are white.

Table 2
Experimental details.

clofarabine	
Crystal data	
Chemical formula	C ₁₀ H ₁₁ ClFN ₅ O ₃
<i>M_r</i>	303.68
Crystal system, space group	Orthorhombic, <i>P</i> ₂ ₁ ₂ ₁
Temperature (K)	295
<i>a</i> , <i>b</i> , <i>c</i> (Å)	5.067481 (12), 10.79402 (2), 22.34124 (5)
<i>V</i> (Å ³)	1222.03 (1)
<i>Z</i>	4
Radiation type	Synchrotron, λ = 0.46873 Å
μ (mm ⁻¹)	0.04
Specimen shape, size (mm)	Cylinder, 2.0 × 1.5
Data collection	
Diffractometer	11-BM, APS
Specimen mounting	Kapton capillary
Data collection mode	Transmission
Scan method	Step
2θ values (°)	2θ _{min} = 0.510, 2θ _{max} = 49.995, 2θ _{step} = 0.001
Refinement	
<i>R</i> factors and goodness of fit	<i>R_p</i> = 0.072, <i>R_{wp}</i> = 0.085, <i>R_{exp}</i> = 0.041, <i>R</i> (<i>F</i> ²) = 0.06753, χ ² = 4.439
No. of parameters	92
No. of restraints	56
(Δ/ <i>σ</i>) _{max}	13.147

Computer programs: *GSAS-II* (Toby & Von Dreele, 2013) and *DIAMOND* (Brandenburg & Putz, 2025).

spherical harmonic model for preferred orientation was included. The texture index was 1.017, indicating that the preferred orientation was slight in this rotated capillary specimen.

4. Database survey

A reduced cell search in the Cambridge Structural Database (CSD, 2026.1.0; Groom *et al.*, 2016), combined with the chemistry C, H, Cl, F, N, and O only, yielded no hits.

5. Synthesis and crystallization

Clofarabine is a commercial reagent, purchased from TargetMol (Batch #132343), and was used as-received.

6. Refinement

Crystal data, data collection and structure refinement details are summarized in Table 2. The white powder was packed into a 1.5 mm diameter Kapton capillary, and rotated during the measurement at ~50 Hz. The powder pattern was measured at 295 K at beam line 11-BM (Lee *et al.*, 2008; Wang *et al.*, 2008; Antao *et al.*, 2008) of the Advanced Photon Source at Argonne National Laboratory using a wavelength of 0.4687342 Å from 0.5–50° 2θ with a step size of 0.001° and a counting time of 0.1 sec step⁻¹. The high-resolution powder diffraction data were collected using twelve silicon crystal analyzers that allow for high angular resolution, high preci-

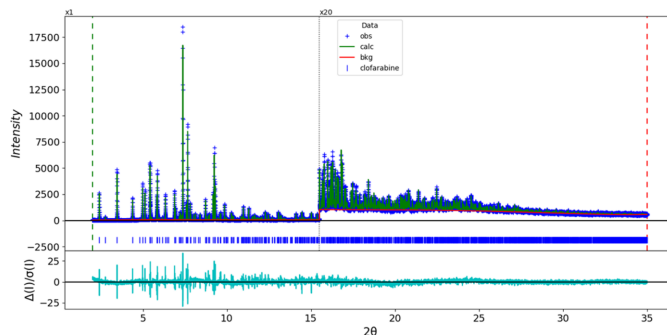


Figure 8

The Rietveld plot for clofarabine. The blue crosses represent the observed data points, and the green line is the calculated pattern. The cyan curve is the normalized error plot, and the red line is the background curve. The blue tick marks indicate the peak positions. The vertical scale has been multiplied by a factor of 20× for 2θ > 15.5°.

sion, and accurate peak positions. A mixture of silicon (NIST SRM 640c) and alumina (NIST SRM 676a) standards (ratio Al₂O₃:Si = 2:1 by weight) was used to calibrate the instrument and refine the monochromatic wavelength used in the experiment.

The pattern was indexed on a primitive orthorhombic unit cell with *a* = 5.06685, *b* = 10.79310, *c* = 22.33892 Å, *V* = 1225.6 Å³, and *Z* = 4 using *N-TREOR* as incorporated into *EXPO2014* (Altomare *et al.*, 2013). The suggested space group was *P*₂₁₂₁, which was confirmed by the successful solution and refinement of the structure.

The molecular structure of clofarabine was downloaded from PubChem (Kim *et al.*, 2023) as Conformer3D_COMPOUND_CID_119182.sdf. It was converted to a *.mol2 file using *Mercury* (Macrae *et al.*, 2020), and to a Fenske–Hall *Z*-matrix using *OpenBabel* (O’Boyle *et al.*, 2011). The structure was solved using parallel tempering techniques as implemented in *FOX* (Favre-Nicolin & Černý, 2002).

Rietveld refinement was carried out using *GSAS-II* (Toby & Von Dreele, 2013). Only the 2.0–35.0° portion of the pattern was included in the refinements (*d*_{min} = 0.779 Å). All non-H bond distances and angles were subjected to restraints, based on a *Mercury* Mogul geometry check (Sykes *et al.*, 2011; Bruno *et al.*, 2004). The Mogul average and standard deviation for each quantity were used as the restraint parameters. The aromatic fused ring system was restrained to be planar. The restraints contributed 1.4% to the overall χ². The hydrogen atoms were included in calculated positions, which were recalculated during the refinement using *Materials Studio* (Dassault Systèmes, 2025). The Cl atom was refined anisotropically. The other *U*_{iso}(H) values were grouped by chemical similarity. The peak profiles were described using the generalized microstrain model (Stephens, 1999). The background was modeled using a six-term shifted Chebyshev polynomial, with a peak at 5.89° to model the scattering from the Kapton capillary and any amorphous component of the sample.

The final refinement of 92 variables using 33,001 observations and 56 restraints yielded the residuals *R*_{wp} = 0.0856 and GOF = 2.11. The largest peak (0.65 Å from Cl1) and hole (0.36 Å from Cl1) in the difference-Fourier map are 0.459 (12)

and $-0.594(12) e \text{ \AA}^{-3}$, respectively. The final Rietveld plot is shown in Fig. 8. The largest features in the normalized error plot are in the positions and shapes of some of the strong low-angle peaks, and may indicate a change in the specimen during the measurement.

The crystal structure of clofarabine was optimized (fixed experimental unit cell) with density functional theory techniques using *VASP* (Kresse & Furthmüller, 1996) through the *MedeA* graphical interface (Materials Design, 2024). The calculation was carried out on 32 cores of a 144-core (768 Gb memory) HPE Superdome Flex 280 Linux server at North Central College. The calculation used the GGA-PBE functional, a plane wave cutoff energy of 400.0 eV, and a *k*-point spacing of 0.5 \AA^{-1} leading to a $3 \times 2 \times 1$ mesh, and took ~ 8.1 h. Single-point density functional theory calculations (fixed experimental cell) and population analysis were carried out using *CRYSTAL23* (Erba *et al.*, 2023). Fixed experimental cell) and population analysis were carried out using *CRYSTAL17* (Dovesi *et al.*, 2018). The basis sets for the H, C, N and O atoms in the calculation were those of Gatti *et al.* (1994), and those for F and Cl were those of Peintinger *et al.* (2013). The calculations were run on a 3.5 GHz PC using 8 *k*-points and the B3LYP functional, and took ~ 1.4 h.

Acknowledgements

Use of the Advanced Photon Source at Argonne National Laboratory was supported by the U. S. Department of Energy, Office of Science, Office of Basic Energy Sciences, under Contract No. DE-AC02-06CH11357. We thank Saul Lapidus for his assistance in the data collection. We also thank the ICDD team – Megan Rost, Steve Trimble, and Dave Bohnenberger – for their contribution to research, sample preparation, and in-house XRD data collection and verification.

Funding information

Funding for this research was provided by: International Centre for Diffraction Data (grant No. 09-03).

References

- Altomare, A., Cuocci, C., Giovacazzo, C., Moliterni, A., Rizzi, R., Corriero, N. & Falcicchio, A. (2013). *J. Appl. Cryst.* **46**, 1231–1235.
- Antao, S. M., Hassan, I., Wang, J., Lee, P. L. & Toby, B. H. (2008). *Can. Mineral.* **46**, 1501–1509.
- Bernstein, J., Davis, R. E., Shimon, L. & Chang, N. L. (1995). *Angew. Chem. Int. Ed. Eng.* **34**, 1555–1573.
- Bonate, P. L., Arthaud, L., Cantrell, W. R., Stephenson, K., Secrist, J. A. & Weitman, S. (2006). *Nat. Rev. Drug Discov.* **5**, 855–863.
- Brandenburg, K. & Putz, H. (2025). *DIAMOND V 5.1.1*. Crystal Impact, Bonn, Germany.
- Bravais, A. (1866). *Etudes Cristallographiques*. Paris: Gauthier Villars.
- Bruno, I. J., Cole, J. C., Kessler, M., Luo, J., Motherwell, W. D. S., Purkis, L. H., Smith, B. R., Taylor, R., Cooper, R. I., Harris, S. E. & Orpen, A. G. (2004). *J. Chem. Inf. Comput. Sci.* **44**, 2133–2144.
- Dassault Systèmes (2025). *BIOVIA Materials Studio 2026*. BIOVIA, San Diego, USA.
- Donnay, J. D. H. & Harker, D. (1937). *Am. Mineral.* **22**, 446–467.
- Dovesi, R., Erba, A., Orlando, R., Zicovich-Wilson, C. M., Civalleri, B., Maschio, L., Rérat, M., Casassa, S., Baima, J., Salustro, S. & Ki Erba, A., Desmarais, J. K., Casassa, S., Civalleri, B., Donà, L., Bush, I. J., Searle, B., Maschio, L., Daga, L.-E., Cossard, A., Ribaldone, C., Ascricchi, E., Marana, N. L., Flament, J.-P. & Kirtman, B. (2023). *J. Chem. Theory Comput.* **19**, 6891–6932.
- Etter, M. C. (1990). *Acc. Chem. Res.* **23**, 120–126.
- Favre-Nicolin, V. & Černý, R. (2002). *J. Appl. Cryst.* **35**, 734–743.
- Friedel, G. (1907). *Bull. Soc. Française Minéral.* **30**, 326–455.
- Gatti, C., Saunders, V. R. & Roetti, C. (1994). *J. Chem. Phys.* **101**, 10686–10696.
- Groom, C. R., Bruno, I. J., Lightfoot, M. P. & Ward, S. C. (2016). *Acta Cryst.* **B72**, 171–179.
- Hirshfeld, F. L. (1977). *Theoret. Chem. Acta* **44**, 129–138.
- Kabekkodu, S., Dosen, A. & Blanton, T. N. (2024). *Powder Diffr.* **39**, 47–59.
- Kaduk, J. A., Crowder, C. E., Zhong, K., Fawcett, T. G. & Suchomel, M. R. (2014). *Powder Diffr.* **29**, 269–273.
- Kim, S., Chen, J., Cheng, T., Gindulyte, A., He, J., He, S., Li, Q., Shoemaker, B. A., Thiessen, P. A., Yu, B., Zaslavsky, L., Zhang, J. & Bolton, E. E. (2023). *Nucleic Acids Res.* **51**, D1373–D1380.
- Kresse, G. & Furthmüller, J. (1996). *Comput. Mat. Sci.* **6**, 15–50.
- Lee, P. L., Shu, D., Ramanathan, M., Preissner, C., Wang, J., Beno, M. A., Von Dreele, R. B., Ribaud, L., Kurtz, C., Antao, S. M., Jiao, X. & Toby, B. H. (2008). *J. Synch. Rad.* **15**, 427–432.
- Macrae, C. F., Sovago, I., Cottrell, S. J., Galek, P. T. A., McCabe, P., Pidcock, E., Platings, M., Shields, G. P., Stevens, J. S., Towler, M. & Wood, P. A. (2020). *J. Appl. Cryst.* **53**, 226–235.
- Materials Design. (2024). *MedeA 3.7.2*. Materials Design Inc., San Diego, USA.
- MDI (2026). *JADE Pro version 9.5*. Materials Data, Livermore, USA.
- Montgomery, J. A. & Secrist, J. A. (1991). United States Patent 5,034,518.
- Montgomery, J. A. & Secrist, J. A. (1997). United States Patent 5,661,136.
- Motherwell, W. D. S., Shields, G. P. & Allen, F. H. (2000). *Acta Cryst.* **B56**, 857–871.
- O’Boyle, N. M., Banck, M., James, C. A., Morley, C., Vandermeersch, T. & Hutchison, G. R. (2011). *J. Chem. Informatics* **3**, 33.
- Peintinger, M. F., Vilela Oliveira, D. & Bredow, T. (2013). *J. Comput. Chem.* **34**, 451–459.
- Silk Scientific. (2013). *UN-SCAN-IT 7.0*. Silk Scientific Corporation, Orem, USA.
- Spackman, P. R., Turner, M. J., McKinnon, J. J., Wolff, S. K., Grimwood, D. J., Jayatilaka, D. & Spackman, M. A. (2021). *J. Appl. Cryst.* **54**, 1006–1011.
- Stephens, P. W. (1999). *J. Appl. Cryst.* **32**, 281–289.
- Streek, J. van de & Neumann, M. A. (2014). *Acta Cryst.* **B70**, 1020–1032.
- Sykes, R. A., McCabe, P., Allen, F. H., Battle, G. M., Bruno, I. J. & Wood, P. A. (2011). *J. Appl. Cryst.* **44**, 882–886.
- Toby, B. H. & Von Dreele, R. B. (2013). *J. Appl. Cryst.* **46**, 544–549.
- Wang, J., Toby, B. H., Lee, P. L., Ribaud, L., Antao, S. M., Kurtz, C., Ramanathan, M., Von Dreele, R. B. & Beno, M. A. (2008). *Rev. Sci. Instr.* **79**, 085105.
- Wavefunction (2025). *Spartan ’24. V. I.3.1*. Wavefunction Inc., Irvine, USA.
- Wheatley, A. M. & Kaduk, J. A. (2019). *Powder Diffr.* **34**, 35–43.
- Xia, C., Zhang, X., Deng, Y., Miao, W. & Tao, Y. (2011). Chinese Patent CN101497640A.

supporting information

Acta Cryst. (2026). E82, 883-887 [https://doi.org/10.1107/S2056989026006584]

Crystal structure of clofarabine (form I), $C_{10}H_{11}ClFN_5O_3$, from synchrotron power diffraction data and density functional theory calculations

Jacob K. Salazar, James A. Kaduk, Anja Dosen and Thomas N. Blanton

Computing details

2-Chloro-9-(2-deoxy-2-fluoro- β -D-arabinofuranosyl)-9H-purin-6-amine (clofarabine)

Crystal data

$C_{10}H_{11}ClFN_5O_3$
 $M_r = 303.68$
 Orthorhombic, $P2_12_12_1$
 $a = 5.067481$ (12) Å
 $b = 10.79402$ (2) Å
 $c = 22.34124$ (5) Å
 $V = 1222.03$ (1) Å³

$Z = 4$
 $D_x = 1.651$ Mg m⁻³
 Synchrotron radiation, $\lambda = 0.46873$ Å
 $\mu = 0.04$ mm⁻¹
 $T = 295$ K
 cylinder, 2.0×1.5 mm

Data collection

11-BM, APS
 diffractometer
 Specimen mounting: Kapton capillary

Data collection mode: transmission
 Scan method: step
 $2\theta_{\min} = 0.510^\circ$, $2\theta_{\max} = 49.995^\circ$, $2\theta_{\text{step}} = 0.001^\circ$

Refinement

Least-squares matrix: full
 $R_p = 0.072$
 $R_{wp} = 0.085$
 $R_{exp} = 0.041$
 $R(F^2) = 0.06753$
 49486 data points
 Profile function: Finger-Cox-Jephcoat function
 parameters U, V, W, X, Y, SH/L: peak
 variance(Gauss) = $U \tan(\text{Th})^2 + V \tan(\text{Th}) + W$;
 peak HW(Lorentz) = $X / \cos(\text{Th}) + Y \tan(\text{Th})$;
 SH/L = S/L + H/L U, V, W in (centideg)², X & Y
 in centideg 1.163, -0.126, 0.063, 0.000, 0.000,
 0.002,
 92 parameters

56 restraints
 16 constraints
 Weighting scheme based on measured s.u.'s
 $(\Delta/\sigma)_{\max} = 13.147$
 Background function: Background function:
 "chebyshev-1" function with 6 terms: 42.46(6),
 -8.82(9), -9.57(8), 2.83(8), -1.00(7), 2.56(7),
 Background peak parameters: pos, int, sig, gam:
 5.889(10), 4.22(8)e3, 4.12(15)e3, 0.100,
 Preferred orientation correction: Simple
 spherical harmonic correction Order = 2
 Coefficients: 0:0:C(2,0) = -0.2134(29);
 0:0:C(2,2) = 0.199(4)

Fractional atomic coordinates and isotropic or equivalent isotropic displacement parameters (Å²)

	x	y	z	$U_{\text{iso}}^*/U_{\text{eq}}$
Cl1	0.0189 (2)	0.16598 (9)	0.02919 (5)	0.0491
F2	0.8827 (3)	0.21882 (16)	0.24051 (9)	0.0404 (4)*
O3	0.3887 (4)	0.0218 (2)	0.29218 (10)	0.0404 (4)*

O4	0.8336 (4)	0.1997 (2)	0.38062 (10)	0.0404 (4)*
O5	0.7624 (5)	-0.1464 (2)	0.33800 (11)	0.0543 (8)*
N6	0.5950 (5)	0.0280 (2)	0.19828 (9)	0.0276 (3)*
N7	0.8275 (5)	-0.1145 (2)	0.14655 (11)	0.0276 (3)*
N8	0.3110 (5)	0.1027 (2)	0.11892 (10)	0.0276 (3)*
N9	0.3786 (5)	-0.0050 (2)	0.02505 (9)	0.0276 (3)*
N10	0.7125 (5)	-0.1486 (2)	0.01227 (11)	0.0276 (3)*
C11	0.4845 (5)	0.1019 (2)	0.24741 (11)	0.0404 (4)*
C12	0.7673 (5)	0.1167 (3)	0.33294 (12)	0.0404 (4)*
C13	0.6750 (5)	0.1895 (2)	0.27873 (12)	0.0404 (4)*
C14	0.5214 (6)	0.0417 (3)	0.34917 (13)	0.0404 (4)*
C15	0.5802 (7)	-0.0816 (3)	0.37589 (16)	0.0543 (8)*
C16	0.5031 (5)	0.0297 (3)	0.14087 (9)	0.0276 (3)*
C17	0.7914 (6)	-0.0585 (3)	0.19924 (11)	0.0276 (3)*
C18	0.6444 (6)	-0.0584 (3)	0.11009 (10)	0.0276 (3)*
C19	0.5783 (6)	-0.0731 (3)	0.04870 (10)	0.0276 (3)*
C20	0.2718 (6)	0.0791 (3)	0.06104 (11)	0.0276 (3)*
H21	0.30900	0.14393	0.23107	0.0526*
H22	0.93174	0.06037	0.32382	0.0526*
H23	0.57838	0.27853	0.28915	0.0526*
H24	0.38326	0.09796	0.37362	0.0526*
H25	0.40893	-0.13251	0.38656	0.0706*
H26	0.68813	-0.06089	0.41746	0.0706*
H27	0.89907	-0.08325	0.23913	0.0358*
H28	0.97473	0.25980	0.36946	0.0526*
H29	0.75868	-0.23048	0.35566	0.0706*
H30	0.66866	-0.15293	-0.03273	0.0358*
H31	0.82978	-0.21654	0.02850	0.0358*

Atomic displacement parameters (Å²)

	U^{11}	U^{22}	U^{33}	U^{12}	U^{13}	U^{23}
C11	0.0463 (9)	0.0535 (9)	0.0474 (10)	0.0085 (15)	-0.0268 (15)	0.0218 (16)

Geometric parameters (Å, °)

C11—C20	1.740 (2)	C14—C12	1.529 (3)
F2—C13	1.392 (2)	C14—C15	1.489 (3)
O3—C11	1.408 (3)	C14—H24	1.076 (3)
O3—C14	1.456 (3)	C15—O5	1.435 (4)
O4—C12	1.432 (3)	C15—C14	1.489 (3)
O4—H28	0.997 (2)	C15—H25	1.055 (4)
O5—C15	1.435 (4)	C15—H26	1.101 (4)
O5—H29	0.990 (2)	C16—N6	1.365 (2)
N6—C11	1.468 (3)	C16—N8	1.345 (2)
N6—C16	1.365 (2)	C16—C18	1.375 (2)
N6—C17	1.364 (2)	C17—N6	1.364 (2)
N7—C17	1.336 (3)	C17—N7	1.336 (3)

N7—C18	1.375 (2)	C17—H27	1.079 (2)
N8—C16	1.345 (2)	C18—N7	1.375 (2)
N8—C20	1.333 (2)	C18—C16	1.375 (2)
N9—C19	1.357 (2)	C18—C19	1.421 (3)
N9—C20	1.328 (2)	C19—N9	1.357 (2)
N10—C19	1.338 (3)	C19—N10	1.338 (3)
N10—H30	1.031 (2)	C19—C18	1.421 (3)
N10—H31	1.011 (2)	C20—C11	1.740 (2)
C11—O3	1.408 (3)	C20—N8	1.333 (2)
C11—N6	1.468 (3)	C20—N9	1.328 (2)
C11—C13	1.522 (2)	H21—C11	1.064 (3)
C11—H21	1.064 (3)	H22—C12	1.052 (3)
C12—O4	1.432 (3)	H23—C13	1.103 (3)
C12—C13	1.518 (2)	H24—C14	1.076 (3)
C12—C14	1.529 (3)	H25—C15	1.055 (4)
C12—H22	1.052 (3)	H26—C15	1.101 (4)
C13—F2	1.392 (2)	H27—C17	1.079 (2)
C13—C11	1.522 (2)	H28—O4	0.997 (2)
C13—C12	1.518 (2)	H29—O5	0.990 (2)
C13—H23	1.103 (3)	H30—N10	1.031 (2)
C14—O3	1.456 (3)	H31—N10	1.011 (2)
C11—O3—C14	111.81 (18)	C12—C13—H23	114.8 (2)
C12—O4—H28	112.9 (2)	O3—C14—C12	104.3 (2)
C15—O5—H29	101.5 (3)	O3—C14—C15	108.1 (3)
C11—N6—C16	124.40 (19)	C12—C14—C15	113.9 (3)
C11—N6—C17	129.7 (2)	O3—C14—H24	103.1 (2)
C16—N6—C17	105.86 (14)	C12—C14—H24	110.6 (3)
C17—N7—C18	103.30 (17)	C15—C14—H24	115.5 (3)
C16—N8—C20	110.43 (17)	O5—C15—C14	109.2 (3)
C19—N9—C20	115.96 (16)	O5—C15—H25	114.1 (3)
C19—N10—H30	120.8 (2)	C14—C15—H25	113.1 (3)
C19—N10—H31	121.5 (2)	O5—C15—H26	106.1 (3)
H30—N10—H31	116.3 (2)	C14—C15—H26	104.9 (3)
O3—C11—N6	109.2 (2)	H25—C15—H26	108.9 (3)
O3—C11—C13	105.89 (15)	N6—C16—N8	126.72 (15)
N6—C11—C13	116.1 (2)	N6—C16—C18	106.42 (13)
O3—C11—H21	102.6 (3)	N8—C16—C18	126.86 (15)
N6—C11—H21	107.12 (19)	N6—C17—N7	113.30 (17)
C13—C11—H21	115.0 (2)	N6—C17—H27	123.5 (2)
O4—C12—C13	110.0 (2)	N7—C17—H27	123.1 (3)
O4—C12—C14	110.2 (3)	N7—C18—C16	111.09 (15)
C13—C12—C14	102.26 (17)	N7—C18—C19	132.98 (18)
O4—C12—H22	108.7 (2)	C16—C18—C19	115.92 (15)
C13—C12—H22	112.9 (3)	N9—C19—N10	118.15 (19)
C14—C12—H22	112.7 (3)	N9—C19—C18	119.43 (17)
F2—C13—C11	109.8 (2)	N10—C19—C18	122.37 (19)
F2—C13—C12	112.0 (2)	C11—C20—N8	113.75 (17)

C11—C13—C12	103.89 (15)	C11—C20—N9	114.91 (16)
F2—C13—H23	105.51 (19)	N8—C20—N9	131.13 (19)
C11—C13—H23	110.9 (2)		

(clofarabine_VASP)

*Crystal data*C₁₀H₁₁ClFN₅O₃ $M_r = 360.68$ Orthorhombic, $P2_12_12_1$ $a = 5.06687 \text{ \AA}$ $b = 10.79280 \text{ \AA}$ $c = 22.33879 \text{ \AA}$ $V = 1221.61 \text{ \AA}^3$ $Z = 4$ $D_x = 1.651 \text{ Mg m}^{-3}$ *Data collection* $h = \rightarrow$ $l = \rightarrow$ $k = \rightarrow$ *Fractional atomic coordinates and isotropic or equivalent isotropic displacement parameters (\AA^2)*

	x	y	z	$B_{\text{iso}}^*/B_{\text{eq}}$
Cl1	0.01212	0.16968	0.02898	
F2	0.90535	0.21606	0.23899	
O3	0.38561	0.02587	0.29060	
O4	0.84115	0.19497	0.38208	
O5	0.75419	-0.14849	0.34117	
N6	0.59832	0.02849	0.19629	
N7	0.81396	-0.11960	0.14513	
N8	0.31324	0.10597	0.11693	
N9	0.37245	-0.00306	0.02375	
N10	0.68616	-0.15566	0.00827	
C11	0.49010	0.10293	0.24534	
C12	0.77245	0.11804	0.33283	
C13	0.69128	0.18783	0.27665	
C14	0.52255	0.04396	0.34742	
C15	0.57085	-0.08032	0.37626	
C16	0.50115	0.03082	0.13866	
C17	0.78576	-0.06389	0.19766	
C18	0.63647	-0.06134	0.10719	
C19	0.56958	-0.07502	0.04585	
C20	0.26192	0.07985	0.05972	
H21	0.33140	0.15735	0.22472	
H22	0.93523	0.05413	0.32150	
H23	0.59644	0.27638	0.28803	
H24	0.39549	0.09995	0.37712	
H25	0.37979	-0.12899	0.38061	
H26	0.64633	-0.06322	0.42197	
H27	0.88790	-0.08940	0.23872	
H28	0.97473	0.25980	0.36946	
H29	0.75849	-0.23464	0.35654	
H30	0.65698	-0.14890	-0.03741	

H31 0.85246 -0.20128 0.02116

Hydrogen-bond geometry (Å, °)

<i>D—H...A</i>	<i>D—H</i>	<i>H...A</i>	<i>D...A</i>	<i>D—H...A</i>
O4—H28...N7 ⁱ	1.01	1.72	2.726	173
O5—H29...N8 ⁱⁱ	0.99	1.86	2.831	167
N10—H30...O4 ⁱⁱⁱ	1.03	1.87	2.854	159
N10—H31...N10 ^{iv}	1.02	2.38	3.271	145
C11—H21...F2 ^v	1.10	2.27	3.208	142
C11—H21...O5 ^{vi}	1.10	2.60	3.531	142
C12—H22...O3 ^{vii}	1.10	2.40	3.396	149
C15—H26...C11 ^{viii}	1.11	2.77	3.570	129
C17—H27...F2 ^{ix}	1.09	2.40	3.177	127

Symmetry codes: (i) $-x+2, y+1/2, -z+1/2$; (ii) $-x+1, y-1/2, -z+1/2$; (iii) $-x+3/2, -y, z-1/2$; (iv) $x+1/2, -y-1/2, -z$; (v) $x-1, y, z$; (vi) $-x+1, y+1/2, -z+1/2$; (vii) $x+1, y, z$; (viii) $-x+1/2, -y, z+1/2$; (ix) $-x+2, y-1/2, -z+1/2$.